

MTP FILE COPY

41

AD-A212 263

TECHNICAL REPORT BRL-TR-3031

BRL

THE EFFECT OF A RIGID ELLIPTICAL INCLUSION
ON A STRAIGHT CRACK

E. M. PATTON
M. H. SANTARE, U OF Delaware

AUGUST 1989

DTIC
ELECTE
SEP 12 1989
S E D

APPROVED FOR PUBLIC RELEASE; DISTRIBUTION UNLIMITED.

U.S. ARMY LABORATORY COMMAND

BALLISTIC RESEARCH LABORATORY
ABERDEEN PROVING GROUND, MARYLAND

89 9 12 047

DESTRUCTION NOTICE

Destroy this report when it is no longer needed. DO NOT return it to the originator.

Additional copies of this report may be obtained from the National Technical Information Service, U.S. Department of Commerce, Springfield, VA 22161.

The findings of this report are not to be construed as an official Department of the Army position, unless so designated by other authorized documents.

The use of trade names or manufacturers' names in this report does not constitute indorsement of any commercial product.

UNCLASSIFIED

SECURITY CLASSIFICATION OF THIS PAGE

REPORT DOCUMENTATION PAGE

Form Approved
OMB No. 0704-0188

1a. REPORT SECURITY CLASSIFICATION UNCLASSIFIED			1b. RESTRICTIVE MARKINGS		
2a. SECURITY CLASSIFICATION AUTHORITY			3. DISTRIBUTION / AVAILABILITY OF REPORT APPROVED FOR PUBLIC RELEASE; DISTRIBUTION UNLIMITED		
2b. DECLASSIFICATION / DOWNGRADING SCHEDULE			5. MONITORING ORGANIZATION REPORT NUMBER(S)		
4. PERFORMING ORGANIZATION REPORT NUMBER(S) BRL-TR- 3031			7a. NAME OF MONITORING ORGANIZATION		
6a. NAME OF PERFORMING ORGANIZATION USA Ballistic Research Lab		6b. OFFICE SYMBOL (if applicable) SLCBR-IB-M	7b. ADDRESS (City, State, and ZIP Code)		
6c. ADDRESS (City, State, and ZIP Code) Aberdeen Proving Ground, MD 21005-5066			9. PROCUREMENT INSTRUMENT IDENTIFICATION NUMBER		
8a. NAME OF FUNDING / SPONSORING ORGANIZATION		8b. OFFICE SYMBOL (if applicable)	10. SOURCE OF FUNDING NUMBERS		
8c. ADDRESS (City, State, and ZIP Code)			PROGRAM ELEMENT NO.	PROJECT NO.	TASK NO.
			WORK UNIT ACCESSION NO.		
11. TITLE (Include Security Classification) The Effect of a Rigid Elliptical Inclusion on a Straight Crack					
12. PERSONAL AUTHOR(S) E.M. Patton and M.H. Santare					
13a. TYPE OF REPORT TR		13b. TIME COVERED FROM _____ TO _____		14. DATE OF REPORT (Year, Month, Day) August 1989	
15. PAGE COUNT					
16. SUPPLEMENTARY NOTATION					
17. COSATI CODES			18. SUBJECT TERMS (Continue on reverse if necessary and identify by block number)		
FIELD	GROUP	SUB-GROUP	Cracks; Fracture Mechanics; Singular Integral Equations, Greens Functions; Stress Analysis of Cracks		
19. ABSTRACT (Continue on reverse if necessary and identify by block number) The general problem of a straight crack near a rigid elliptical inclusion is solved. Complex potentials presented in a previous paper for the interaction of an edge dislocation with rigid ellipse are used to formulate the Green's function for this problem. The solution is written as a set of singular integral equations for crack opening displacement that are solved numerically. Stress intensity factors are presented for a variety of crack/inclusion geometries.					
20. DISTRIBUTION / AVAILABILITY OF ABSTRACT <input type="checkbox"/> UNCLASSIFIED/UNLIMITED <input checked="" type="checkbox"/> SAME AS RPT. <input type="checkbox"/> DTIC USERS			21. ABSTRACT SECURITY CLASSIFICATION UNCLASSIFIED		
22a. NAME OF RESPONSIBLE INDIVIDUAL Edward M. Patton			22b. TELEPHONE (Include Area Code) (301) 278-6805		22c. OFFICE SYMBOL SLCBR-IB-M

CONTENTS

	<u>Page</u>
LIST OF FIGURES	v
ACKNOWLEDGEMENTS	vii
1. INTRODUCTION	1
2. METHOD OF SOLUTION	2
3. RESULTS AND CONCLUSIONS	6
4. REFERENCES	12
DISTRIBUTION	13

Accession For	
NTIS GRA&I	<input checked="" type="checkbox"/>
DTIC TAB	<input type="checkbox"/>
Unannounced	<input type="checkbox"/>
Justification	
By _____	
Distribution/	
Availability Codes	
Sist	Avail and/or Special
A-1	



LIST OF FIGURES

<u>Figure</u>	<u>Page</u>
1. Problem geometry	2
2. Mapping function -- crack geometry in Z-plane mapped to unit circle in W-plane . . .	3
3. Stress intensity factor versus distance from ellipse for a radially oriented crack and varying aspect ratios (M), $L = 1.0/R$	7
4. Stress intensity factor versus alpha for a radial crack and various aspect ratios, $L = 1.0/R$, $d = 0.1/R$	7
5. Stress intensity factor versus distance for aspect ratio of 0.8 and small alpha, $L = 1.0/R$	8
6. Stress intensity factor versus distance for aspect ratio of 0.9 and small alpha, $L = 1.0/R$	8
7. Stress intensity factor versus alpha for varying aspect ratios (0.8 to 1.0) with crack constant distance from origin, ($Z_1 = 2.1/R$), $L = 1.0/R$	9
8. Stress intensity factor versus distance from Y-axis for vertical and horizontal crack ($\theta = 0$ or 90), $L = 1.0/R$, $Y_1 = 0.5/R$	9

ACKNOWLEDGMENTS

The authors would like to gratefully acknowledge the support of the University of Delaware Research Foundation and the Center for Composite Materials, and the U.S. Army Ballistic Research Laboratory.

1. INTRODUCTION

The interaction between inclusions and cracks has been an active field of study for many years. Applications of the results of theoretical analyses have wide implications in the implementation of a broad range of new and emerging material systems. The understanding gained by the solution of appropriate elasticity problems allows researchers to gain insight into the mechanisms of strengthening and toughening, as well as material damage, because of the presence of material defects. The mechanisms of crack growth in composite materials and ceramics, and that of strain hardening in metal alloys, are primary examples of the direct application of the results of the study of crack interaction.

The problem of the interaction between a circular inclusion and a crack has been solved by Atkinson¹ for a radial crack and by Erdogan, Gupta, and Ruwani² for an arbitrarily oriented crack. Erdogan and Gupta³ later solved the problem in which the crack crosses the interface. These solutions are based on the Green's function solutions consisting of a dislocation interacting with a circular inclusion (Dundurs and Mura⁴ and Dundurs and Sendeckyj).⁵ In an earlier paper, Santare and Keer,⁶ presented the two-dimensional solution for the dislocation outside a rigid elliptical inclusion. The problem was solved using the complex potential methods of Muskhelishvili.⁷ Special attention was paid to the rotation of the elliptical inclusion and the effect that has on the stress field around the ellipse. Results were compared with a power series solution found by Stagni and Lizzio,⁸ which did not take into account the rotation of the ellipse. The comparison showed that the rotation has a significant effect on the stress field in many instances. In another paper, Santare, Keer, and Lewis⁹ solved a related problem of an elliptical hole at a bone/implant interface, with symmetrical cracks radiating from the edges of the ellipse, along the x-axis. Solutions to the resulting singular integral equations were found using a numerical scheme proposed by Gerasoulis.¹⁰

This paper provides the numerical solution of the general problem of a straight crack near a rigid elliptical inclusion. The problem is formulated using the results of Reference 6 and the numerical technique used in Reference 9. The ellipse can be made to have any shape, from a circular inclusion to a line inclusion. The crack is oriented at an arbitrary angle to the x-axis, with the length of the crack, $L = |z_2 - z_1|$. The geometry of the problem is shown in Figure 1.

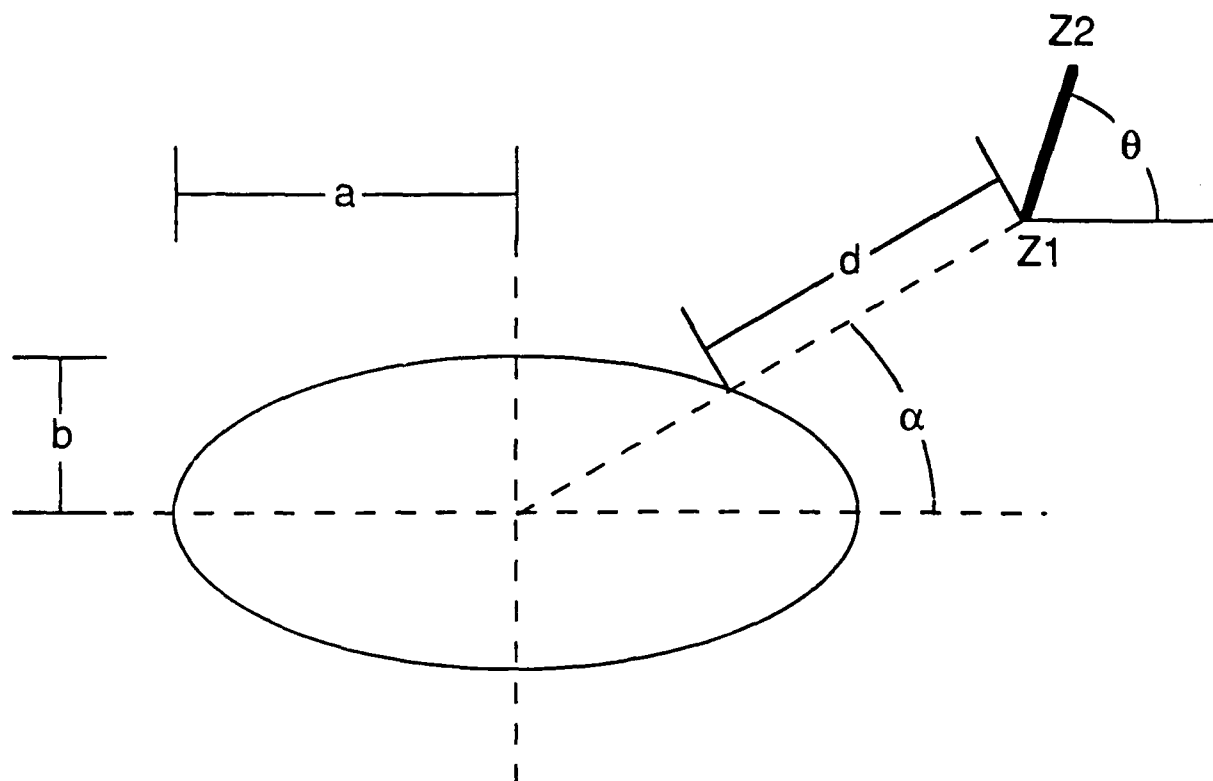


Figure 1. Problem geometry.

2. METHOD OF SOLUTION

The problem is posed in terms of the complex potentials of Mushkhelishvili,⁷ in which stresses and displacements can be written in terms of two analytic functions as follows:

$$\sigma_{xx} + \sigma_{yy} = 2 [\phi'(z) + \overline{\phi'(z)}] \quad (1)$$

$$\sigma_{yy} - \sigma_{xx} + 2i \sigma_{xy} = 2 [\bar{z} \phi''(z) + \psi'(z)] \quad (2)$$

$$2\mu (u+iv) = \kappa \phi(z) - z \overline{\phi'(z)} - \overline{\psi(z)} \quad (3)$$

where $z = x + iy$, μ is the shear modulus of the matrix material, $\kappa = 3 + 4\nu$ for plane strain, and $\kappa = (3 - \nu)/(1 + \nu)$ for plane stress, where ν is the poisson's ratio for the matrix. The prime notation is understood as the derivative with respect to z , and the superimposed bar denotes the complex conjugate.

The geometry of the problem is simplified by using the function that maps the region outside the ellipse onto the region outside the unit circle, as shown in Figure 2. This mapping can be written as,

$$z = \omega(\zeta) = R \left(\zeta + \frac{m}{\zeta} \right) \quad (4)$$

where

$$R = \frac{a + b}{2},$$

$$m = \frac{a - b}{a + b}$$

and a and b are shown in Figure 1.

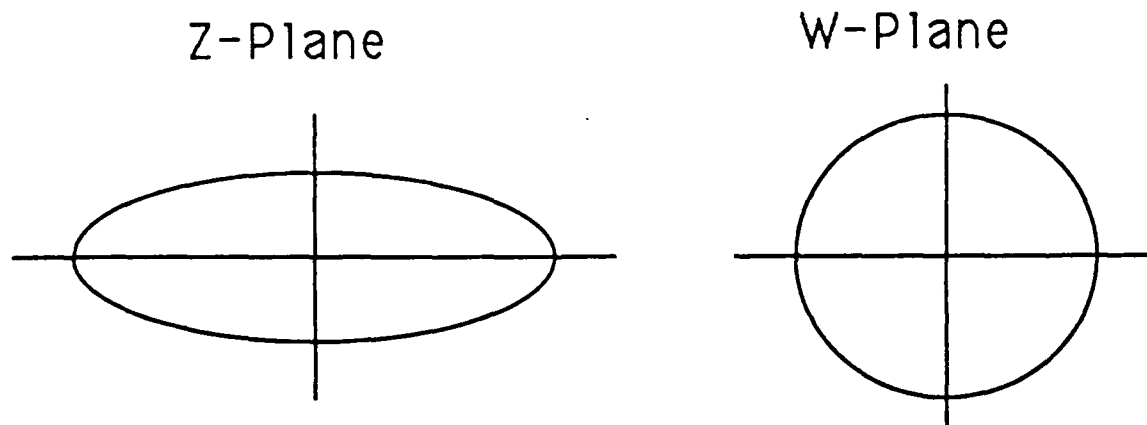


Figure 2. Mapping function -- crack geometry in Z-plane mapped to unit circle in W-plane.

The solution for a dislocation interacting with a rigid elliptical inclusion is used as a Green's function for the crack problem. The potentials were derived in Reference 6 and are restated here for convenience. They include the dislocation in the form of $\gamma = \mu (b_x + ib_y)/\pi (\kappa + 1)$, the mapped coordinates ζ and ζ_0 , which are the transformed z and z_0 , and the rotation of the ellipse ϵ_0 .

$$\begin{aligned} \phi(\zeta) = & \frac{\gamma}{\kappa} \log [R(\zeta - \zeta_0 + m/\zeta - m/\zeta_0)] \\ & + \log [(\zeta - 1/\bar{\zeta}_0)/\zeta] - \gamma \log [(\zeta - m/\zeta_0)/\zeta] \\ & - \frac{\gamma}{\kappa m} \frac{(1/\bar{\zeta}_0 - m/\zeta_0)(1/\bar{\zeta}_0 - \zeta_0)}{(1/\bar{\zeta}_0 - \bar{\zeta}_0/m)(1/\bar{\zeta}_0 - \zeta)} + 2\mu i \epsilon_0 R m/\kappa \zeta \end{aligned} \quad (5)$$

$$\begin{aligned} \psi(\zeta) = & \gamma \log [R(\zeta - \zeta_0 + m/\zeta - m/\zeta_0)] - \gamma \frac{\bar{\zeta}_0 + m/\bar{\zeta}_0}{\zeta - \zeta_0 + m/\zeta - m/\zeta_0} \\ & + \kappa \bar{\gamma} \log [(\zeta - 1/\bar{\zeta}_0)/\zeta] - \bar{\gamma} \log [(\zeta - m/\zeta_0)/\zeta] \\ & + \gamma m \frac{(m/\zeta_0 - 1/\bar{\zeta}_0)(m/\zeta_0 - \bar{\zeta}_0/m)}{(m/\zeta_0 - \zeta_0)(m/\zeta_0 - \zeta)} + 2\mu i \epsilon_0 R/\zeta \\ & - \zeta \frac{1 + m\zeta^2}{\zeta^2 - m} \left[\frac{\gamma}{\kappa} \frac{1/\bar{\zeta}_0}{\zeta(\zeta - 1/\bar{\zeta}_0)} - \gamma \frac{m/\zeta_0}{\zeta(\zeta - m/\zeta_0)} \right. \\ & \left. + \frac{\gamma}{\kappa m} \frac{(1/\bar{\zeta}_0 - m/\zeta_0)(1/\bar{\zeta}_0 - \zeta_0)}{(1/\bar{\zeta}_0 - \bar{\zeta}_0/m)(\zeta - 1/\bar{\zeta}_0)^2} - \mu \epsilon_0 m/\kappa \zeta^2 \right] \end{aligned} \quad (6)$$

where

$$\begin{aligned} \epsilon_0 = \operatorname{Re} i \left[-\kappa \bar{\gamma} / \bar{\zeta}_0 + \bar{\gamma} m / \zeta_0 + \gamma m^2 / \zeta_0 \right. \\ \left. - \gamma m / \kappa \bar{\zeta}_0 - \gamma m \frac{(m / \zeta_0 - 1 / \bar{\zeta}_0) (m \zeta_0 - \bar{\zeta}_0 / m)}{(m / \bar{\zeta}_0 - \zeta_0)} \right. \\ \left. + \frac{\bar{\gamma}}{\kappa} \frac{(1 / \bar{\zeta}_0 - m / \bar{\zeta}_0) (1 \zeta_0 - \zeta_0)}{(1 / \bar{\zeta}_0 - \bar{\zeta}_0 / m)} \right] / 2 \mu R \left(1 + \frac{m^2}{\kappa} \right) \end{aligned} \quad (7)$$

The first term in ϕ and the first two terms in ψ represent the potentials for dislocation in an unbounded medium. These terms, when applied to equations (1) and (2) to calculate the stresses, become singular, as $1/\sqrt{z-z_0}$. The remainder of the terms in both potentials account for the interaction between the ellipse and the dislocation. These terms, when used in equations (1) and (2), constitute the nonsingular stresses due to the interaction between the dislocation and the inclusion. Note also that the rotation of the ellipse is taken into account through these nonsingular terms and is called ϵ_0 . The last term in the expression for ψ (the bracketed terms) contains the first derivative of the interaction portion of the first potential ϕ . This is a natural consequence of the method of Mushkhelishvili.⁷

Summing these stresses along the crack length, and setting them equal to the stresses due to the external load, two singular integral equations result. The solution of these equations will give us the distribution of dislocations along the crack. If we resolve the stresses into components normal to the crack (Mode I), and along the crack (Mode II), the two equations can be stated as follows:

$$\int_{z_1}^{z_2} \frac{b_n}{z - z_0} dz_0 + \int_{z_1}^{z_2} \sigma_n(z, z_0) b_n(z_0) dz_0 = f_n(z) \quad (8)$$

$$\int_{z_1}^{z_2} \frac{b_t}{z - z_0} dz_0 + \int_{z_1}^{z_2} \sigma_t(z, z_0) b_t(z_0) dz_0 = f_t(z) \quad (9)$$

where the n and t subscripts refer to the normal and tangential components with respect to the crack, and f_n and f_t are the stresses due to the external load. The first term in each of these equations

represents the Cauchy singular portion of the stresses (as noted above), and the second term contains the nonsingular parts. The normal and tangential cartesian stress components can be determined using a standard trigonometric transformation. Furthermore, if equations (8) and (9) are rewritten in terms of $|z-z_0| e^{i\theta}$, one can determine the stress due to the Cauchy singular portion of the above integral equation, in terms of the angle θ (the angle of the crack), as follows:

$$\sigma_{yy} = \frac{1}{|z-z_0|} [b_y (\cos \theta + \cos 3 \theta) - b_x (3 \sin \theta + \sin 3 \theta)] \quad (10)$$

$$\sigma_{xx} = \frac{1}{|z-z_0|} [b_y (3 \cos \theta - \cos 3 \theta) - b_x (\sin 3 \theta - \sin \theta)] \quad (11)$$

$$\sigma_{xy} = \frac{1}{|z-z_0|} [b_y (\sin 3 \theta - \sin \theta) + b_x (\cos 3 \theta + \cos \theta)] \quad (12)$$

The technique used to solve for the unknown distribution of dislocations was developed by Gerasoulis.¹⁰ He uses a piecewise, quadratic, polynomial representation of the singular and nonsingular parts of the integral equation to discretize the equation into a set of algebraic expressions suited for a matrix-type solution. In order to solve the equation, we must first make an assumption about the nature of the singularity at the tips of the crack. Because the crack is contained entirely in the matrix material, the stresses at both crack tips will be singular, as $1/\sqrt{z-z_0}$. The dislocation density, therefore, will also exhibit square-root singularity at both tips and can be rewritten in the following form:

$$b(t) = g(t) / \sqrt{1-t^2} \quad (13)$$

where $t = 2(z-z_1)/(z_2-z_1) - 1$. The functions $g(t)$ are continuous and bounded on the interval $t \in [-1, 1]$. For a given n , this integral is broken into $2n+1$ integration points and $2n$ collocation points. Gerasoulis¹⁰ states that the method works equally well for unequal meshes, but in this problem an equal spacing of the integration and collocation points is used. Convergence in this problem is relatively good using this method. A value of n above 6 was unnecessary for crack lengths on the order of the size of the inclusion.

3. RESULTS AND CONCLUSIONS

Figures 3 through 8 are given in an attempt to compare and contrast the present results with those found by Atkinson¹ and Erdogan, et al.,² for the circular inclusion and with Grief and Sanders¹¹ for a line inclusion. In the last of these papers, the integral equation is formulated somewhat differently and

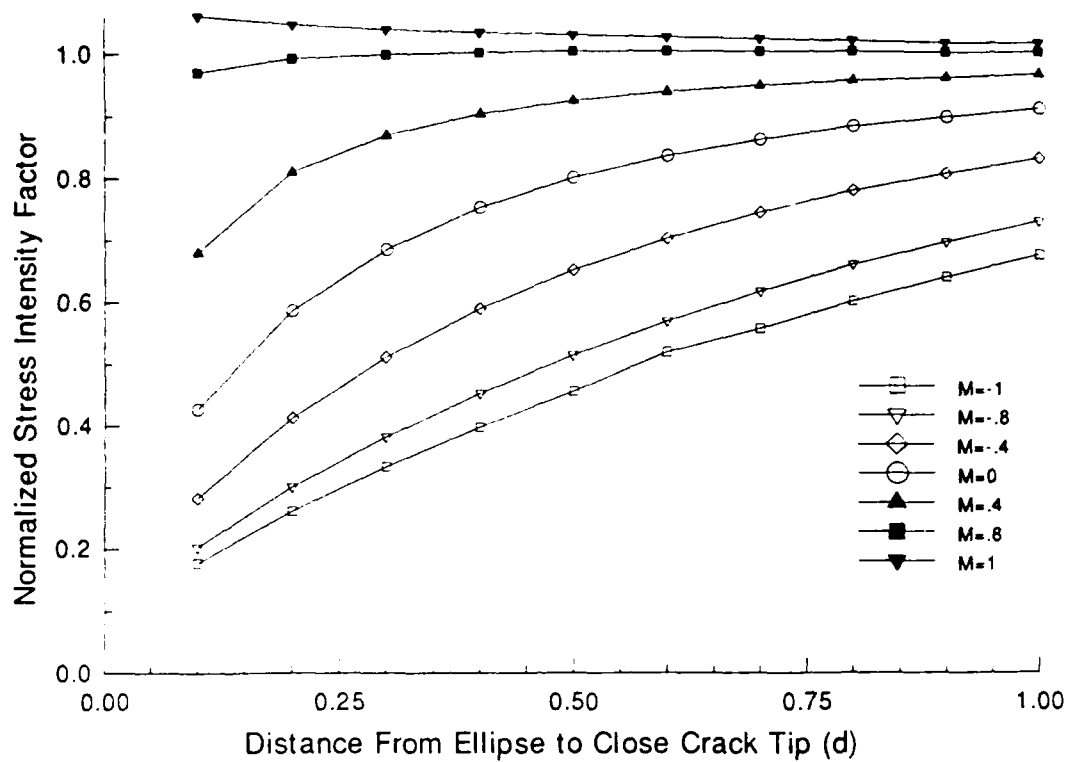


Figure 3. Stress intensity factor versus distance from ellipse for a radially oriented crack and varying aspect ratios (M). $L = 1.0/R$.

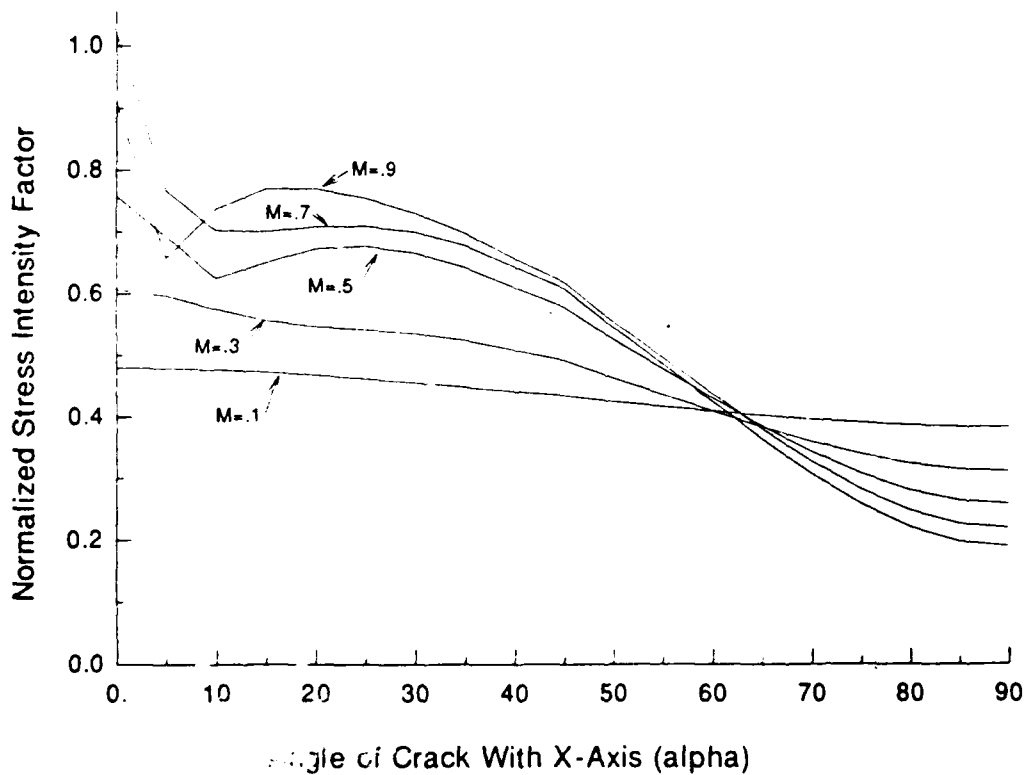


Figure 4. Stress intensity factor versus alpha for a radial crack and various aspect ratios. $L = 1.0/R$, $d = 0.1/R$.

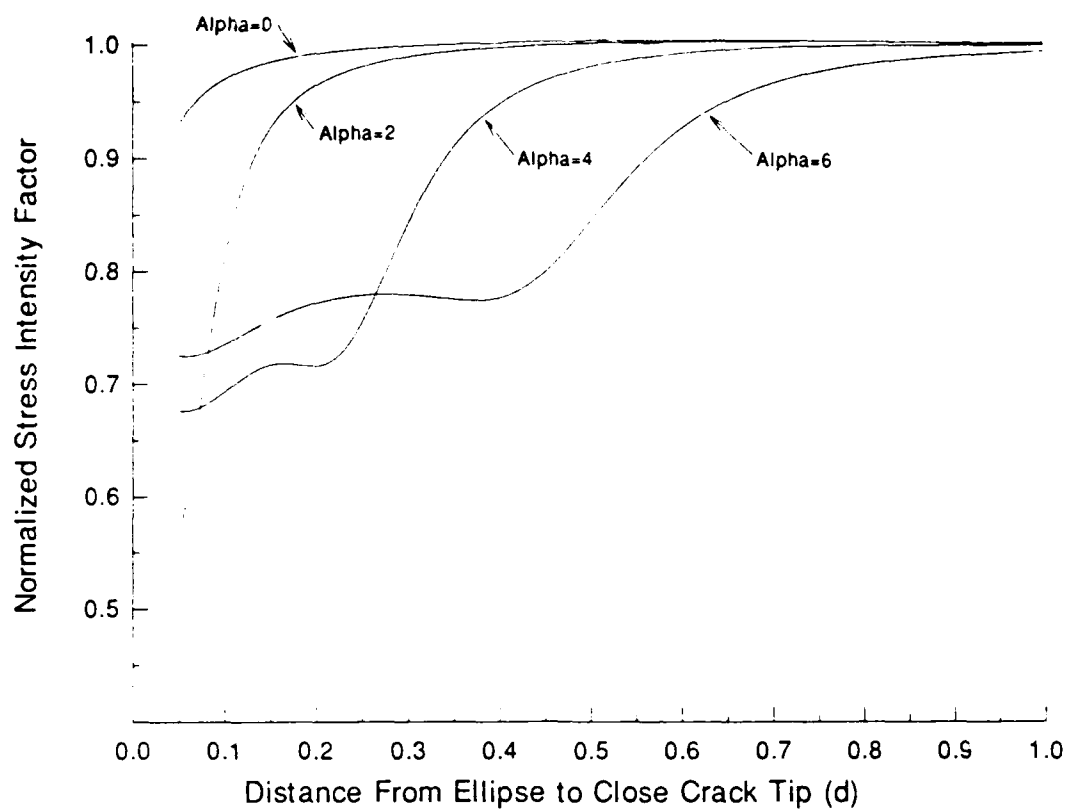


Figure 5. Stress intensity factor versus distance for aspect ratio of 0.8 and small alpha, $L = 1.0/R$.

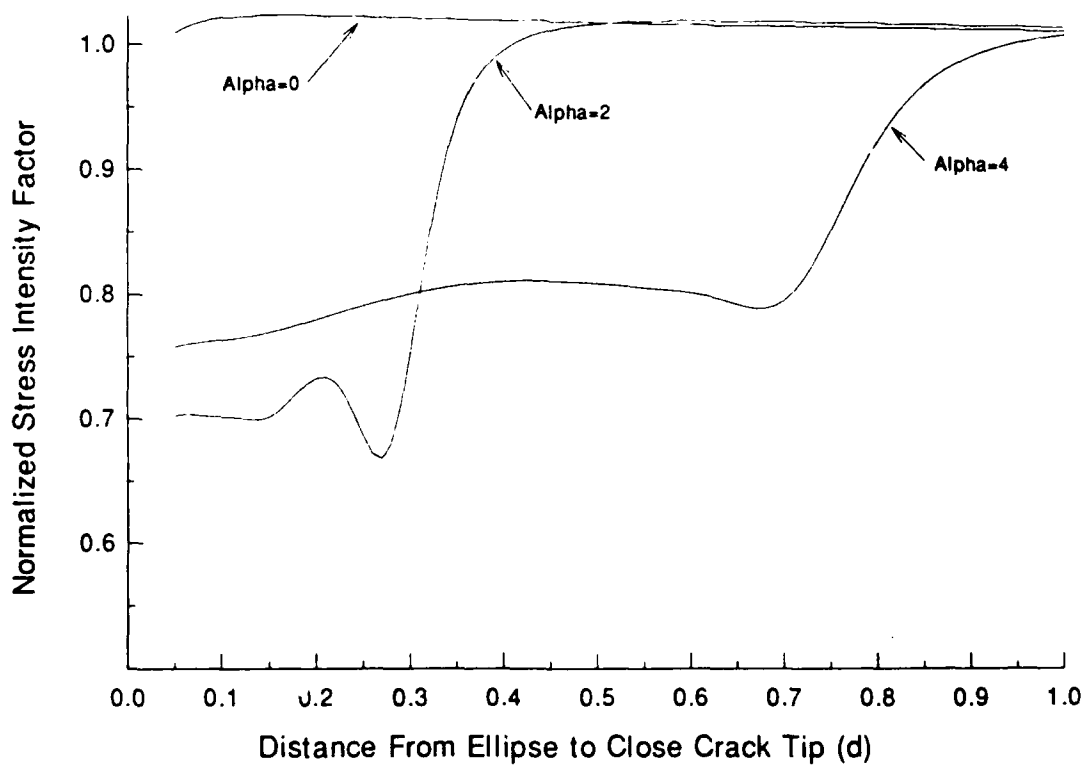


Figure 6. Stress intensity factor versus distance for aspect ratio of 0.9 and small alpha, $L = 1.0/R$.

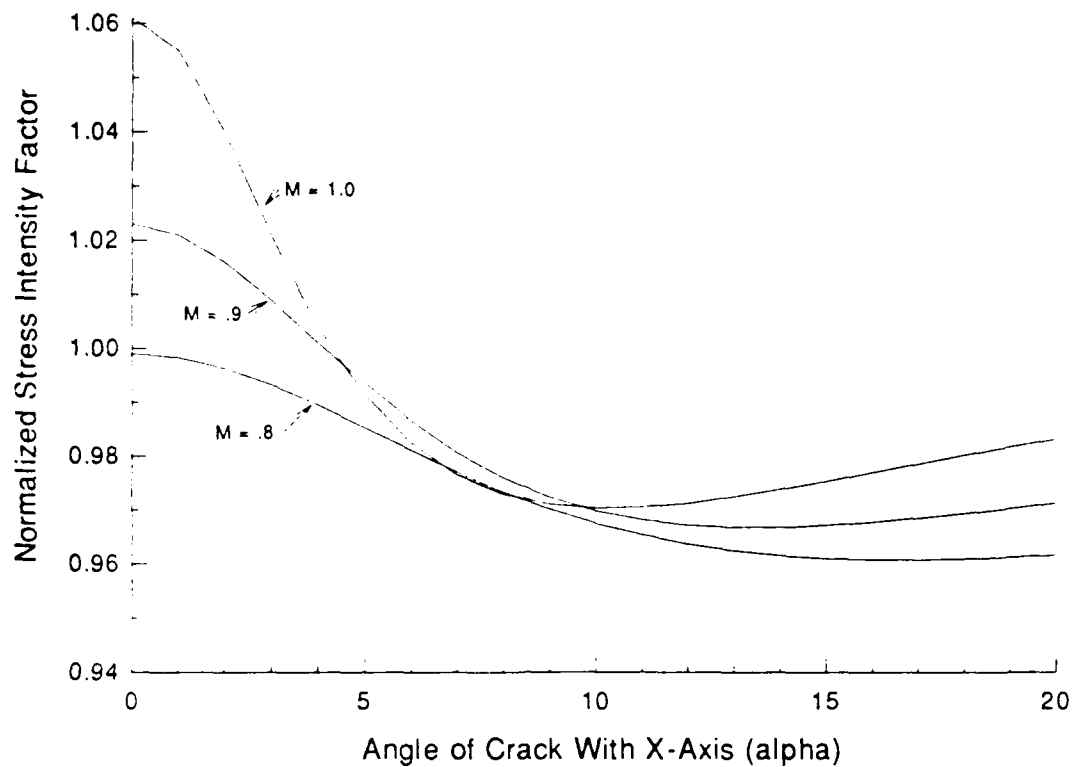


Figure 7. Stress intensity factor versus alpha for varying aspect ratios (0.8 to 1.0) with crack constant distance from origin, ($Z1 = 2.1/R$), $L = 1.0/R$.

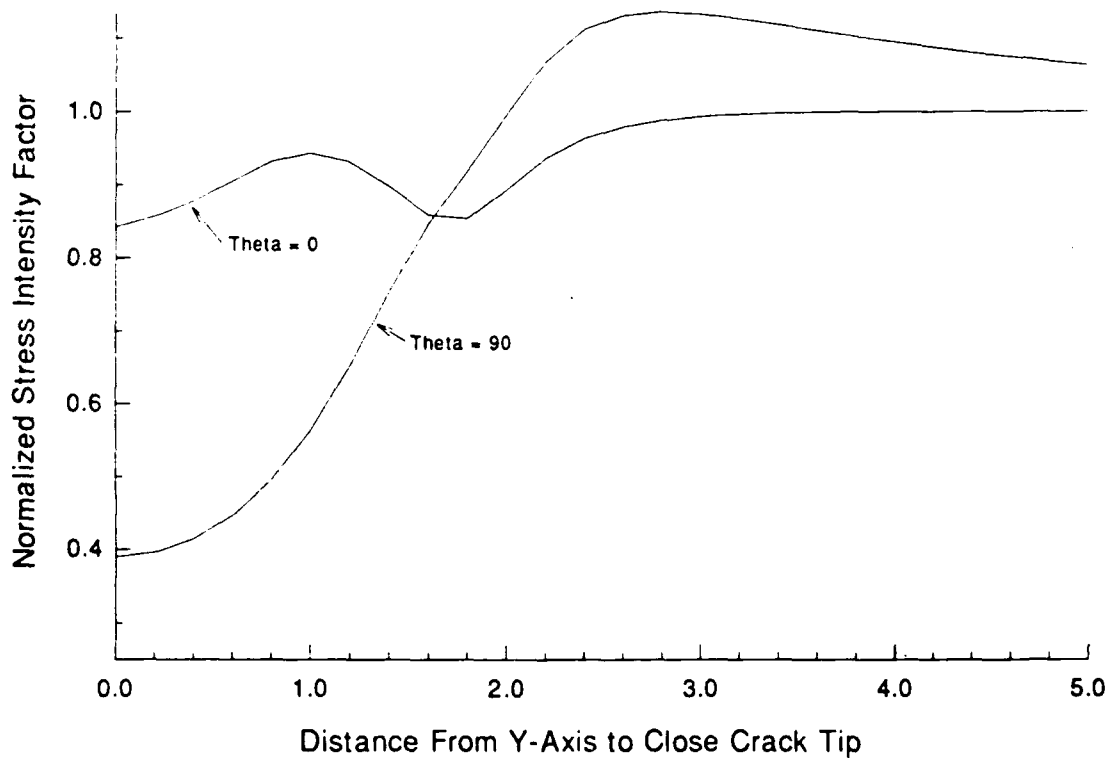


Figure 8. Stress intensity factor versus distance from Y-axis for vertical and horizontal crack ($\theta = 0$ or 90), $L = 1.0/R$, $Y1 = 0.5/R$.

corresponds only to the interaction terms in the current problem. The present solution takes into account both the interaction terms and the stress singularities associated with the crack, in the same form as Atkinson¹ and as Erdogan and Gupta.³ In Figures 3 through 7, the crack is radially oriented with respect to the origin, that is θ is equal to α . Figure 8 presents results for a crack in which θ and α are not equal.

Figure 3 is a plot of the normalized mode I stress intensity factor $K_I/\sigma \sqrt{L}$ versus the distance from the close tip of the crack to the inclusion for several elliptical shapes (m varying from 0 to 1), with the angle α either equal to 0 or 90° (along the x-axis or the y-axis). Note that the stress intensity factor is lowest when approaching the crack from the side, ($\alpha = 90^\circ$) as would be expected. An interesting result is shown in Figure 4, in which normalized stress intensity factor is plotted against α for varying elliptical aspect ratios. The only parameters varied in this figure are α and the aspect ratio of the ellipse. The distance from the close tip of the crack to the ellipse and the crack length are kept constant. The close tip of the crack is 0.1/R from the ellipse, and the normalized crack length (L/R) is taken as 1. Note that, for relatively flat ellipses ($m > .5$), the location of the close tip of the crack varies rapidly with small changes in angle α . In effect, once the crack rotates slightly from the x-axis, it is shielded by the flat side of the ellipse, and the stress intensity factor drops rapidly. Figures 5 and 6 illustrate this in more detail. In these figures, stress intensity factor is plotted against distance from the ellipse for small α . Figure 5 shows the results for an ellipse with an aspect ratio of 0.8, and Figure 6 shows the same for an ellipse of 0.9 aspect ratio.

In Figure 7, a different approach is taken. In this figure, the close tip of the crack is a fixed distance from the origin, rather than from the ellipse, and the angle α is varied from 0 to 20° for different aspect ratios of the ellipse. The normalized distance from the origin to the close tip of the crack in this figure is 2.1/R. For an α of 0°, and an ellipse with an aspect ratio of 1, this is equivalent to having the crack 0.1/R from the ellipse. Note in Figure 7 that, for all angles, the stress intensity factor is very close to unity. This is contrasted with about a 25 to 30 percent decrease of stress intensity factor for these small values of α when the crack is shielded by the ellipse, as shown in Figures 5 and 6.

This effect has broad implications in the modeling of toughening mechanisms in brittle materials. It seems that a crack at the end of a small, thin inclusion would be likely to grow, whereas a crack oriented normal to the major axis of an elliptical inclusion would be less likely to grow. Orientation of the inclusions--as well as their shape--must, therefore, be taken into account in the toughening models.

Figure 8 presents results for a crack that is not radially oriented. In this figure, the crack is oriented either horizontally ($\theta = 0^\circ$) or vertically ($\theta = 90^\circ$), while the y-coordinate of the close tip of the crack (z_1) is kept at a value of 0.5. The crack length is maintained at a constant value of $1.0/R$, and the x-coordinate of the close tip of the crack (x_1) is varied from 0 to a value of $3.0/R$, for an elliptical aspect ratio of 0.8. Note that the crack becomes unshielded at a distance of approximately $1.80/R$ from the y-axis. With the crack oriented horizontally, the stress intensity factor dips slightly, as the close tip of the crack (z_1) approaches the end of the ellipse. For a vertical crack, the stress intensity factor passes near unity at this point and rises to a value significantly above 1. The interaction with the ellipse is still evident for this crack at a large distance from the ellipse.

The technique presented in this paper is extremely flexible in nature, as there are several parameters that can be varied independently, and in combination with each other, to produce interesting and useful results. Consequently, there is an infinite number of possibilities that could be explored. This paper has presented just a few of those possible results. The parameters varied in this study were chosen in an attempt to compare this formulation with previously published results.

4. REFERENCES

1. Atkinson, C., "The Interaction Between a Crack and an Inclusion," International Journal of Engineering Science, Vol. 10, pp. 127-136, 1972.
2. Erdogan, F., Gupta, G.D., and Ratwani, M., "Interaction Between a Circular Inclusion and an Arbitrarily Oriented Crack," Journal of Applied Mechanics, pp. 1007-1013, 1974.
3. Erdogan, R., Gupta, G.D., "The Inclusion Problem with a Crack Crossing the Boundary," International Journal of Fracture, 1975.
4. Dundurs, J., Mura, T., "Interaction Between an Edge Dislocation and a Circular Inclusion," Journal of Mechanics & Physics of Solids, Vol. 12, pp. 177-189, 1964.
5. Dundurs, J., Sendekyj, G.P., "Edge Dislocation Inside a Circular Inclusion," Journal of Mechanics & Physics of Solids, Vol. 13, pp. 141-147, 1965.
6. Santare, M.H., Keer, L.M., "Interaction Between an Edge Dislocation and a Rigid Elliptical Inclusion," Journal of Applied Mechanics, Vol. 53, pp. 383-385, 1986.
7. Muskhelishvili, N.I., Some Basic Problems in the Mathematical Theory of Elasticity, 3rd Ed., Noordhoff, P., Ltd, Groningen, Holland, 1954.
8. Stagni, L., Lizzio, R., "Shape Effects in the Interaction Between an Edge Dislocation and an Elliptical Inhomogeneity," Applied Physics A30, pp. 217-221, 1983.
9. Santare, M.H., Keer, L.M., and Lewis, J.L., "Cracks Emanating from a Fluid Filled Void Loaded in Compression: Application to the Bone-Implant Interface," Journal of Applied Mechanics, Vol. 109, pp. 55-59, 1987.
10. Gerasoulis, A., "The use of Piecewise Quadratic Polynomials for the Solution of Singular Integral Equations of Cauchy Type," Computations and Mathematics with Applications, Vol. 8, pp. 15-22, 1982.
11. Greif, R., Sanders, J.L., "The Effect of a Stringer on the Stress in a Cracked Sheet," Journal of Applied Mechanics, pp. 59-66, 1965.

BRL MANDATORY DISTRIBUTION LIST

No of Copies	Organization	No of Copies	Organization
(Unclass., unlimited) 12	Administrator	1	Commander
(Unclass., limited) 2	Defense Technical Info Center		US Army Missile Command
(Classified) 2	ATTN: DTIC-DDA		ATTN: AMSMI-RD-CS-R (DOC)
	Cameron Station		Redstone Arsenal, AL 35898-5010
	Alexandria, VA 22304-6145		
1	HQDA (SARD-TR)	1	Commander
	Washington, DC 20310-0001		US Army Tank Automotive Command
			ATTN: AMSTA-TSL (Technical Library)
1	Commander		Warren, MI 48397-5000
	US Army Materiel Command	1	Director
	ATTN: AMCDRA-ST		US Army TRADOC Analysis Command
	5001 Eisenhower Avenue		ATTN: ATAA-SL
	Alexandria, VA 22333-0001		White Sands Missile Range, NM 88002-5502
1	Commander	(Class. only) 1	Commandant
	US Army Laboratory Command		US Army Infantry School
	ATTN: AMSLC-DL		ATTN: ATSH-CD (Security Mgr.)
	Adelphi, MD 20783-1145		Fort Benning, GA 31905-5660
2	Commander	(Unclass. only) 1	Commandant
	Armament RD&E Center		US Army Infantry School
	US Army AMCCOM		ATTN: ATSH-CD-CSO-OR
	ATTN: SMCAR-MSI		Fort Benning, GA 31905-5660
	Picatinny Arsenal, NJ 07806-5000		
2	Commander	1	AFWL/SUL
	Armament RD&E Center		Kirtland AFB, NM 87117-5800
	US Army AMCCOM	(Class. only) 1	The Rand Corporation
	ATTN: SMCAR-TDC		P.O. Box 2138
	Picatinny Arsenal, NJ 07806-5000		Santa Monica, CA 90401-2138
1	Director	1	Air Force Armament Laboratory
	Benet Weapons Laboratory		ATTN: AFATL/DLODL
	Armament RD&E Center		Eglin AFB, FL 32542-5000
	US Army AMCCOM		
	ATTN: SMCAR-LCB-TL		<u>Aberdeen Proving Ground</u>
	Watervliet, NY 12189-4050		Dir, USAMSAA
1	Commander		ATTN: AMXSY-D
	US Army Armament, Munitions		AMXSY-MP, H. Cohen
	and Chemical Command		Cdr, USATECOM
	ATTN: SMCAR-ESP-L		ATTN: AMSTE-TO-F
	Rock Island, IL 61299-5000		Cdr, CRDEC, AMCCOM
			ATTN: SMCCR-RSP-A
1	Commander		SMCCR-MU
	US Army Aviation Systems Command		SMCCR-MSI
	ATTN: AMSAV-DACL		
	4300 Goodfellow Blvd.		
	St. Louis, MO 63120-1798		
1	Director		
	US Army Aviation Research		
	and Technology Activity		
	Ames Research Center		
	Moffett Field, CA 94035-1099		

AUTHORS'
DISTRIBUTION LIST

No. of Copies	Organization
3	Director U.S. Army Material Lab ATTN: SLCMT-MEC (Director) Dr. Halpin Dr. Barsoum Watertown, MA 02171-2719
1	Battelle Pacific Northwest Lab ATTN: Mark Smith P.O. Box 999 Richland, WA 99352
2	Lawrence Livermore Nat'l Lab ATTN: R. Christensen W. Feng Livermore, CA 94550
2	Commander Wright-Patterson Air Force Base AFWAML (Dr. Steve Tsai) Dayton, OH 45433
2	Sandia National Laboratory ATTN: W. Robinson B. Benedetti Livermore, CA 94550
2	David Taylor Research Center ATTN: W. Phyllaier-1720.2 R. Rockwell-1720.2 Bethesda, MD 20054-5000
2	Los Alamos Nat'l Laboratory ATTN: D. Rabern (G-787) Los Alamos, NM 87545
3	Director Benet Weapons Lab, ARDEC ATTN: L. Johnson J. Underwood G. D'Andrea Watervliet Arsenal Watervliet, NY 12189

USER EVALUATION SHEET/CHANGE OF ADDRESS

This laboratory undertakes a continuing effort to improve the quality of the reports it publishes. Your comments/answers below will aid us in our efforts.

1. Does this report satisfy a need? (Comment on purpose, related project, or other area of interest for which the report will be used.) _____

2. How, specifically, is the report being used? (Information source, design data, procedure, source of ideas, etc.) _____

3. Has the information in this report led to any quantitative savings as far as man-hours or dollars saved, operating costs avoided, or efficiencies achieved, etc? If so, please elaborate. _____

4. General Comments. What do you think should be changed to improve future reports? (Indicate changes to organization, technical content, format, etc.) _____

BRL Report Number _____ Division Symbol _____

Check here if desire to be removed from distribution list. _____

Check here for address change. _____

Current address: Organization _____
Address _____

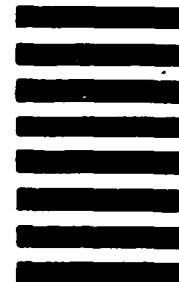
-----FOLD AND TAPE CLOSED-----

Director
U.S. Army Ballistic Research Laboratory
ATTN: SLCBR-DD-T(NEI)
Aberdeen Proving Ground, MD 21005-5066

OFFICIAL BUSINESS
PENALTY FOR PRIVATE USE \$300



NO POSTAGE
NECESSARY
IF MAILED
IN THE
UNITED STATES



Director
U.S. Army Ballistic Research Laboratory
ATTN: SLCBR-DD-T(NEI)
Aberdeen Proving Ground, MD 21005-9989